TECHNICAL REPORT

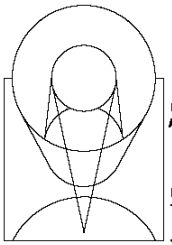

SPACE TELESCOPE SCIENCE INSTITUTE

Operated for NASA by AURA

Title: WFIRST Integral Field Channel Simulation Baselines	Doc #: WFIRST-STScI-TR1701 Date: March 28, 2017 Rev:
Authors: David Law, David Rubin, Klaus Pontoppidan Phone: 410 – 338 - 4803	Release Date:

1 Abstract

The WFIRST mission design includes a low-resolution integral field spectrograph channel (IFC) designed to obtain spatially resolved spectroscopy for supernova observations and galaxy photometric redshift calibration. Accurate simulation tools are a key part of understanding the utility of the IFC for such observations as a component of the WFIRST science program. Here we describe our construction of **three** independently developed simulators that we have used as a crosscheck on each other to ensure both numerical accuracy and a complete understanding of the assumptions inherent in such simulations. We briefly describe these three tools, and demonstrate that they give estimated signal-to-noise ratios that agree to within 1% with each other in four limiting cases from the shot-noise dominated to detector-dominated regimes. This level of agreement strengthens our confidence in the values derived from the simulators as part of a comprehensive science investigation.

2 Introduction

The WFIRST mission will contain as part of its instrument complement a pair of low-resolution integral field spectrographs designed to obtain spatially resolved spectroscopy at resolution R ~ 100 over the wavelength range 0.4 – 2 μm for roughly 3'' x 3'' and 6" x 6" areas of sky. The detailed design of this integral-field channel (hereafter IFC) is driven by the specific requirements of the WFIRST science programs.

The small-field IFU is motivated primarily by the WFIRST dark energy mission, and aims to use IFU spectra of supernovae to constrain fundamental cosmological parameters. The large-field IFU is motivated primarily by the weak lensing program and is intended to obtain spectroscopic calibrators for the WFIRST photometric redshift classification system.

We note that the detailed logic and trade space informing the selection of specific designs for the IFC **using** these tools is beyond the scope of this reference document; for present purposes we state simply that we have assumed a slicer-style design for the IFC with 0.15'' width slices and an H2RG-like detector whose pixels have an angular footprint of 0.075'' on the sky. We note

that these values (along with the detector throughputs, electronic noise characteristics, etc.) are all subject to change, and have indeed evolved between performing the simulations described herein and writing this report.

3 Simulation codes

In order to ensure that any one simulation code is providing realistic results for a given set of inputs it is helpful to compare multiple independently developed codes and ensure that any differences are well understood. Although we demonstrate good agreement between the three codes, we note that they have different interfaces, target different audiences, and differ in the ease of adapting the code to different assumptions.

3.1 Pandeia

JWST and WFIRST will both be supported at STScI by a general-purpose exposure time calculator named Pandeia (Pontoppidan+16) and developed as part of a multi-mission concept. Pandeia is 100% data driven, and new observatories can be implemented by simply modifying a well-defined set of reference files. Pandeia allows detailed scene creation for a broad variety of science cases and constructs fully three-dimensional models of input scenes with two spatial dimensions and one spectral dimension. Pandeia includes detailed detector models with a focus on IR CMOS types that includes the Hawaii 2RG/4RG family under consideration for WFIRST.

The Pandeia simulation tools are designed to be of high production-value, version-controlled, pure python, and well documented As such, they form the backbone of the online exposure time calculators made available by STScI for both the JWST and WFIRST missions.

3.2 D. Law simulation code

D. Law has previously developed IDL-based simulation codes for the Keck/OSIRIS lenslet IFU (Law+06) and the SDSS/MaNGA fiber-based IFU spectrographs (Law+15). These codes have been merged together and adapted for use with the WFIRST slicer-style IFU. Unlike Pandeia, this code is not thoroughly documented or designed for ease of use by a non-expert user. However, it has been proven to work reliably for two current-generation IFU spectrographs, and has the advantage of being flexible and easy to add experimental functionality without the risk of impacting a large user base.

This simulation code is under active version control; the specific version used for the simulations in this document can be found at https://github.com/drlaw1558/wfirst/tree/v20160223

3.3 D. Rubin simulation code

D. Rubin's simulation code (Rubin+17, in prep) is a pure-Python simulator, and simulates both broadband imaging and IFC spectroscopy. It is only partially documented and not intended for general purpose use, but is available at https://github.com/wfirst-sn/wfirst-sim. The motivation for this simulator was to interface with other SN simulation tools developed for the WFIRST

survey, as well as compute intermediate products useful for assessing systematic uncertainties (e.g., PSF-weighted e-/pix/second for assessing the impact of count-rate nonlinearity). As this code is designed to be called repeatedly during a survey simulation, it generates a spectrum simulation in only ~ 0.01 seconds.

4 Input Data and Operating Assumptions

4.1 Input and calibration references

One of the most critical areas in which the WFIRST IFU working group made progress during this project was on the standardization of input files; both in content and in format so that all three simulation tools could ingest identical reference data. Indeed, the authors found that the majority of differences in the performance of the three simulation tools were due to a combination of known and (at the time) unknown differences in the treatment of input spectral sampling, detector noise models, throughput curve normalization, etc.

We discuss each of these further in the following sections, and note that all of the relevant common-format reference files used in the present work can be found at
https://github.com/drlaw1558/wfirst/tree/v20160223/RefFiles

4.2 Common Operating Assumptions

Optical Setup: We assume that the IFC field is composed of 20 slices each of width 0.15 arcsec and length 3.0 arcsec perfectly abutted against each other with zero light loss between the slices. There are no optical distortions, and each slice reformats and disperses light incident upon it onto a different region of the detector in which the spectral dispersion vector runs exactly vertically along the detector columns. Using a pixel scale of 0.075 arcsec/pixel in the along-slice direction, each slice is therefore 40 detector columns in width. The telescope diameter is taken to be 236 cm with an unobscured collecting area of 33680 cm^2.

Wavelength solution and spectral dispersion: Numerous small differences between the initial runs of the three comparison models were tracked down to slight differences in the adopted detector pixel wavelength solution and different interpolation schemes that gave slightly different values even when interpolating a given input with one wavelength solution onto a different common output wavelength solution. It is therefore important to standardize the wavelength solution and dispersion of all input reference files. Our adopted wavelength solution is defined in the FITS binary reference table waifs_prism_disp.fits with columns giving the effective central wavelength (in microns) of each row of detector pixels, the spectral width of the pixel (in microns), and the effective spectral resolution ($R = \lambda/\lambda_{FWHM}$, where λ_{FWHM} is the FWHM of a spectrally unresolved line) at that wavelength.

Throughput: We use the Cycle 5 throughput curves derived by GSFC available at
https://wfirst.gsfc.nasa.gov/science/sdt/wps/references/instrument/WFIRST-WF-Cycle5_throughput_150518.xlsx

These give the effective area as a function of wavelength accounting for the reflectivity of OTE optical surfaces, prism throughput, detector QE, and other relevant factors. In practice, we have used the above file as input to our reference file waifs_throughput.fits which interpolates the Goddard curves to our adopted wavelength solution, and extends the results blueward to 0.4 microns (from 0.6 microns) using a linear taper.

Backgrounds: We assume that the background (or really, foreground) signal corresponds to a combination of zodiacal light and telescope thermal emission. The zodiacal light model (taken from the JWST exposure time calculator as a typical midrange background) is given in MJy/sr in the reference file waifs_zodi_medium.fits. The thermal emission model assumes two 282K sources (corresponding to the primary and secondary mirrors) radiating at 2.5% emissivity that are described as disks placed a focal length away from the focal plane; this model is given in MJy/sr in the reference file waifs_thermal.fits.

Point Spread Function: We use a model of the WFIRST PSF produced by the WebbPSF simulation code. This PSF model is stored in sparse format in the reference file psfcube.fits.gz, which provides realizations of the PSF on a 0.015 arcsec/pixel grid sampled ~ every 0.01 microns. We use linear interpolation from this reference file to construct the effective PSF for our simulations at each spectral channel. In Figure 1 below we show this PSF for reference at 0.4 and 2.0 microns.

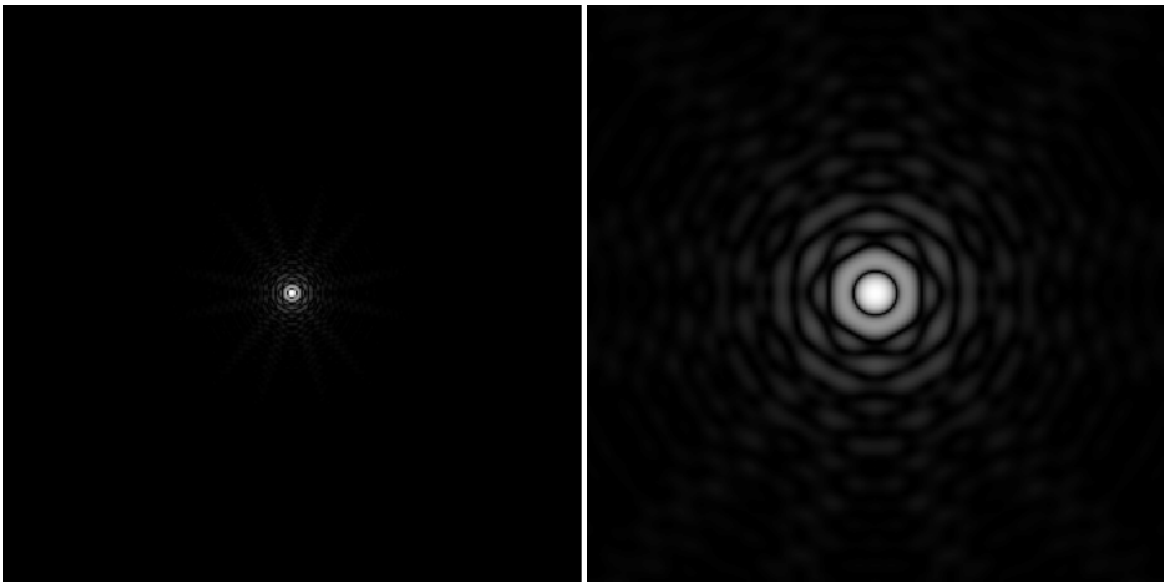

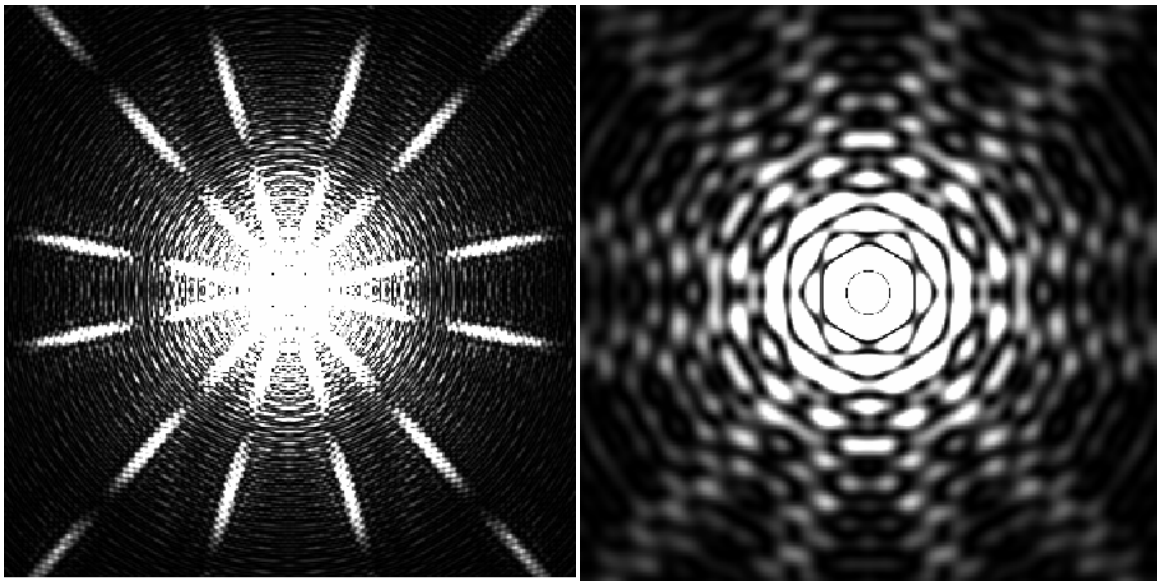

Figure 1 WFIRST PSF inputs from WebbPSF. Left columns show the PSF at 0.4 μm, right columns at 2.0 μm. Top rows use a weak logarithmic stretch while the bottom rows show an extreme linear stretch to illustrate the low-intensity outer structure.

Noise model: We adopt the JWST MULTIACCUM noise model described in Rauscher+2007 and updated in an erratum thereto (Rauscher+2010). Per these references, the total noise variance is given by:

$$\sigma^2_{\text{total}} = \frac{12(n-1)}{mn(n+1)}\sigma^2_{\text{read}} + \frac{6(n^2+1)}{5n(n+1)}(n-1)t_g f - \frac{2(m^2-1)(n-1)}{mn(n+1)}t_f f.$$

where n is the number of groups up the ramp, m is the number of frames per group, σ_{read} is the read noise per frame in e-, t_g is the time (in seconds) between groups, t_f is the time interval between frames, and f is the count rate in units of e-/s/pixel including both astrophysical and dark current. For ease of comparisons to Pandeia, we adopt values comparable to the baseline for the JWST NIRSpec H2RG detectors; m=4, σ_{read} =10 e-, t_f=10.63 seconds, t_g=m*t_f=42.52 seconds, and f_{dark}=0.01 e-/s/pixel (we anticipate, however, that both the frame time and the dark current will be lower for WFIRST). The total integration time for a given exposure is set dynamically as t_{int}=(n-1)*t_g corresponding to effectively quantized total integration times.

Spectral Extraction: There are multiple techniques for extraction of a one-dimensional spectrum from a three-dimensional data cube; for simplicity of comparing the different simulation tools we adopt a simple 0.3'' radius aperture extraction algorithm with no corrections for aperture losses. This is obviously an oversimplification since it will include an undesirably large number of pixel with negligible source flux at 0.4 μm (FWHM ~ 0.04 arcsec) and lose appreciable flux at 2 μm (FWHM ~ 0.2 arcsec) but has the benefit of being an easy assumption to compare across multiple codes.

Neglected Details: We neglect the effects of flat-fielding and other calibration errors, correlated detector noise (e.g., 1/f noise), cosmic rays, and intrapixel capacitance.

5 Simulations

These simulations are chosen not to all be representative of typical WFIRST supernovae spectra, but to span a wide range in possible observations from the detector-limited to shot noise-limited regimes. First we present an overview of the operation of one of the simulation tools in order to give a general context, and then present results for a variety of cases. The operations of the other two simulation tools are similar in concept, but can differ in details.

5.1 Law model logical flow

This code first constructs an input three-dimensional scene with a working angular pixel size of 0.015 arcsec/pixel and a wavelength sampling matched to the adopted WFIRST wavelength solution. This three-dimensional scene is composed of a point source (a single pixel) which is assigned the spectrum of the input science object; all other pixels are assigned corresponding values according to the incident background term (zodiacal plus thermal). These spectra are converted from flux units to units of e-/pixel by multiplying by the usual energy-photon count conversion factor, the telescope effective area vector, the known slice and pixel solid angles, and the specified exposure time. This 3d model is then convolved at each wavelength channel with a model of the WFIRST PSF and sampled by the optical IFU model using a footprint mask for each spatial element (slice and detector pixel), and reformatted into pixels on a mock detector. We determine a corresponding noise value for each detector pixel using the MULTIACCUM noise model accounting for detector, source, and background noise terms.

We combine together the dispersed spectra across an arbitrary number of dithered exposures into a regularly-sampled 3d spectral data cube one wavelength channel at a time using a modified Shepard interpolation algorithm (Law+16) using the known astrometric location of each spatial sample. We assume a reconstructed cube angular pixel size of 0.05 arcsec, and an interpolant with a scale radius of 0.05'' and a region of interest radius of 0.15''. Three such cubes are constructed; one corresponding to a science+noise data cube, one corresponding to a 'noiseless' cube, and a variance cube. We determine the signal-to-noise ratio of an extracted spectrum by performing aperture extraction on the noiseless cube (giving a perfect representation of the signal) and the variance cube (giving a perfect representation of the noise), and using a Monte Carlo approach to account for covariance introduced by the 3d cube rectification algorithm.

5.2 Bright blackbody

Our first example case is for a bright 5000K blackbody source normalized to 19th magnitude in V-band. The input spectrum used is given at waifs_blackbody19.fits

We use a single exposure with n=22 groups for a total integration time of 893 seconds. The source is chosen to be centered in both IFU slice and detector pixel (along slice) location. This example is chosen to test the source-dominated noise regime.

As illustrated in Fig 2, this source is sufficiently bright that it is extremely well detected with a peak SNR of ~130 near 1.2 microns. All three simulation tools agree on the shape and normalization of the SNR curves to within 1%.

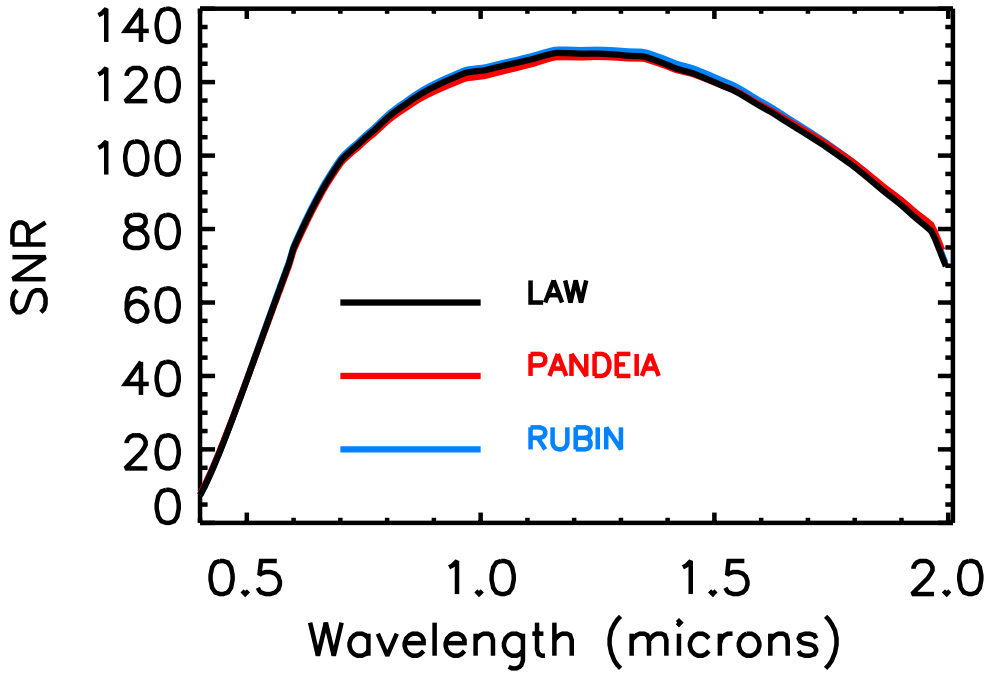

Figure 2 Estimated signal-to-noise ratio for the bright 19th magnitude blackbody example case for the three simulation tools.

5.3 Medium SNR supernova at z=0.5

Our second example case is a single exposure of a typical supernova spectrum located at a redshift z=0.5. The input spectrum used is a Hsiao SN type Ia template (waifs_sn1a_z0.5.fits). We use a single exposure with n=12 groups (t_{int} = 468 seconds) and a source centered in both slice and pixel location. This example is chosen to test mid-range performance in which source, backgrounds, and detector noise all contribute to the resulting SNR.

As illustrated in Figure 3, all three simulation codes again achieve nearly indistinguishable results in the SNR ~ 1-6 regime.

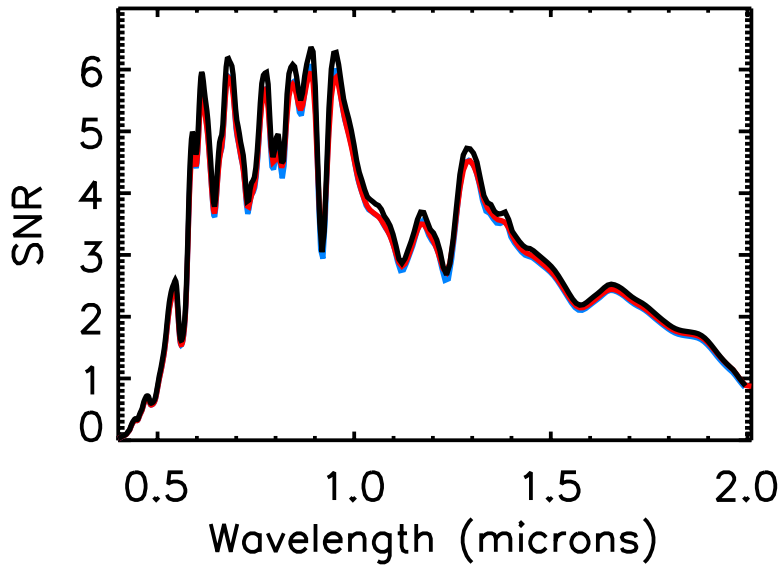

Figure 3 Estimated signal-to-noise ratio for a single 468 second observation of a z =0.5 Type 1A supernova. Colors are as in Figure 2.

5.4 Two-exposure dithered supernova at z=0.5

Our third example case is a dithered exposure of the same z=0.5 supernova (waifs_sn1a_z0.5.fits). This time, we use two exposures, each with n=22 groups (893 seconds), the first with the supernova centered in slice and pixel location and the second with the supernova exactly on the boundary between adjacent slices/pixels. This example is chosen to test the impact of half-integer dithering on the simulation codes (a common technique used to recover spatial resolution from undersampled data).

As illustrated in Figure 4, all three simulation codes again achieve nearly indistinguishable results, peaking at about SNR = 15. Since Figures 3 and 4 are roughly representative of typical SNR that might be expected for real WFIRST supernova observations, we also show in Fig 5 the example simulated spectra resulting from a realization of such SNR characteristics.

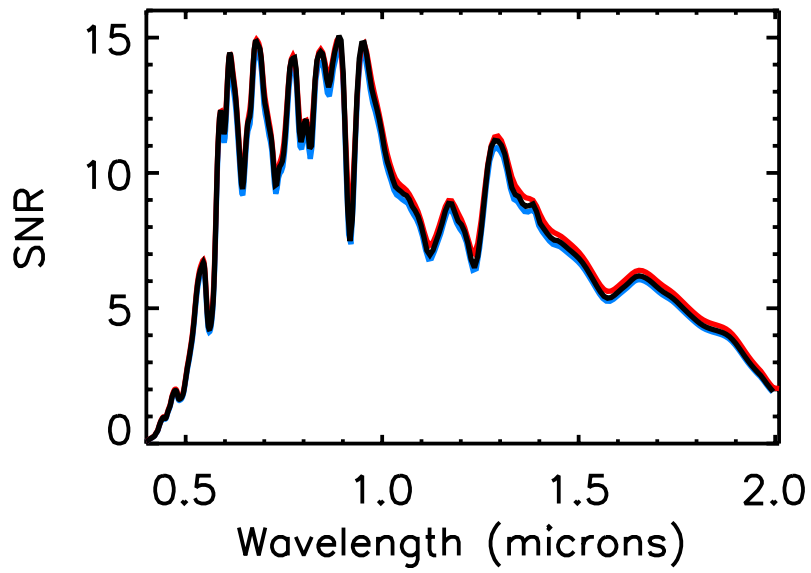

Figure 4 Estimated signal-to-noise ratio for a dithered 1786 second observation of a z =0.5 Type 1A supernova. Colors are as in Figure 2.

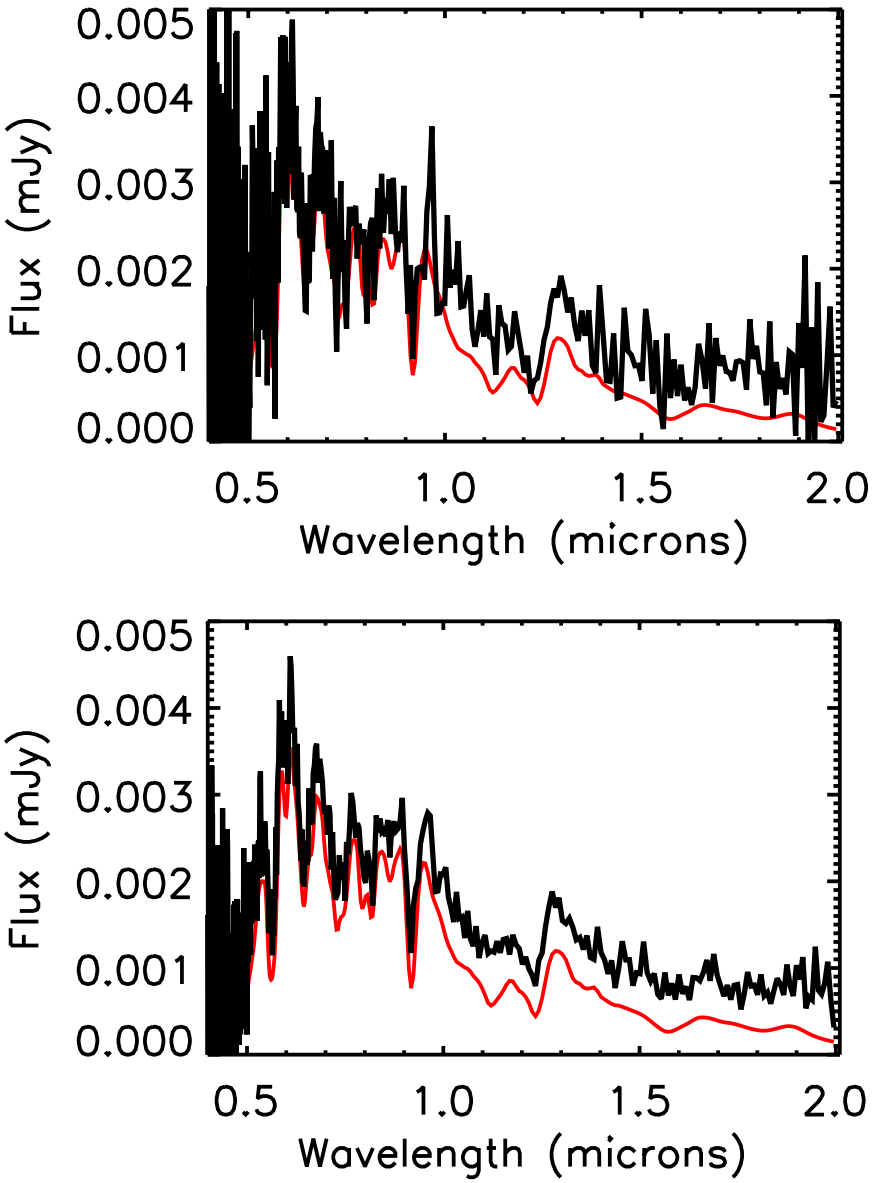

Figure 5 Simulated spectra for a z=0.5 supernova observed for 468 seconds (top panel) and 1786 seconds (bottom panel), corresponding to the SNR curves shown in Figures 3 and 4 respectively. The black line shows the simulated spectrum, the red line indicates the noiseless 'truth' spectrum (offset slightly along the ordinate direction for clarity). Typical WFIRST supernova program spectra are expected to be intermediate between these two cases.

5.5 Low SNR supernova at z=1.5

Our fourth and final example case is a single short exposure of a z=1.5 supernova (waifs_sn1a_z1.5.fits). We choose to use n=12 groups (468 seconds), with the supernova placed exactly on the boundary between adjacent slices/pixels. This example is chosen to test the detector noise characteristics of the simulators by spreading out the light from a faint science

target maximally on the detector.

As illustrated in Figure 6, all three simulation codes again estimate signal-to-noise ratios consistent with each other to within 1%, peaking at about SNR = 1. This confirms that all three codes agree in the detector-limited regime.

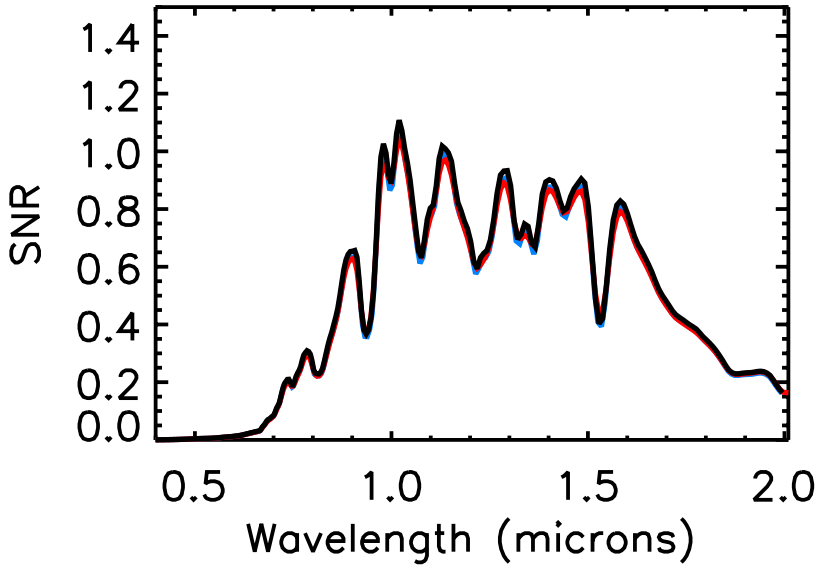

Figure 6 Estimated signal-to-noise ratio for a single 468 second observation of a z =1.5 Type 1A supernova. Colors are as in Figure 2.

6. Conclusions

We have demonstrated that all three simulation tools deliver estimated signal-to-noise ratios that agree to within 1% with each other in four limiting cases from the shot-noise dominated to detector-dominated regimes. Additionally, we have provided input reference data in a standardized format that can be used to test any new simulation tools. The results of these simulations are provided online (https://github.com/drlaw1558/wfirst/tree/v20170328/TR1701) and give a baseline for both the easily-accessible Pandeia simulation tool provided to the community by STScI and for more complex SIT-specific tools developed by the WFIRST science teams for internal use.

Acknowledgements

This work was carried out at Space Telescope Science Institute (STScI) under contract with the WFIRST Project Office at NASA Goddard Space Flight Center (GSFC), in the context of the WFIRST Science Operations Center, which is a partnership between GSFC, STScI, and the Infrared Processing and Analysis Center (IPAC).

References

(1) Law, D.R., Steidel, C.C., and Erb, D.K. 2006, AJ, 131, 70.
"Predictions and Strategies for Integral-Field Spectroscopy of High-Redshift Galaxies."
(2) Law, D.R., et al. 2015, AJ, 150, 19
"Observing Strategy for the SDSS-IV/MaNGA IFU Galaxy Survey"
(3) Law, D.R. et al. 2016, AJ, 152, 83
"The Data Reduction Pipeline for the SDSS-IV MaNGA IFU Galaxy Survey"
(4) Pontoppidan, K. et al. 2016, SPIE, 9910, 16
"Pandeia: a multi-mission exposure time calculator for JWST and WFIRST"
(5) Rauscher, B. et al. 2007, PASP, 119, 768
"Detectors for the James Webb Space Telescope Near-Infrared Spectrograph. I. Readout Mode, Noise Model, and Calibration Considerations"
(6) Rauscher, B. et al. 2010, PASP, 122, 1254
" Erratum"

Law simulation code used for this work:
https://github.com/drlaw1558/wfirst/tree/v20160223

Rubin simulation code used for this work:
https://github.com/wfirst-sn/wfirst-sim

Reference files used for this work:
https://github.com/drlaw1558/wfirst/tree/v20160223/RefFiles

WFIRST system throughput reference table:
https://wfirst.gsfc.nasa.gov/science/sdt/wps/references/instrument/WFIRST-WF-Cycle5_throughput_150518.xlsx

Plotting code and simulation results to reproduce all simulation figures in this technical report:
https://github.com/drlaw1558/wfirst/tree/v20170328/TR1701